Live-attenuated YF17D-vectored COVID-19 vaccine protects from lethal yellow fever virus infection in mouse and hamster models

Ji Ma,[a,b] Michael Bright Yakass,[a,b,c] Sander Jansen,[a,b] Bert Malengier-Devlies,[d] Dominique Van Looveren,[a,b,e] Lorena Sanchez-Felipe,[a,b] Thomas Vercruysse,[a,b,e] Birgit Weynand,[f] Mahadesh Prasad Arkalagud Javarappa,[a,b] Osbourne Quaye,[a,b,c] Patrick Matthys,[d] Tania Roskams,[f] Johan Neyts,[a,b] Hendrik Jan Thibaut,[a,b,e] and Kai Dallmeier[a,b]*

[a]KU Leuven Department of Microbiology, Immunology and Transplantation, Rega Institute, Laboratory of Virology, Molecular Vaccinology and Vaccine Discovery, Leuven, Belgium
[b]Global Virus Network (GVN), Baltimore, MD, USA
[c]West African Centre for Cell Biology of Infectious Pathogens (WACCBIP), Department of Biochemistry, Cell and Molecular Biology, University of Ghana, Legon, Accra, Ghana
[d]KU Leuven Department of Microbiology, Immunology and Transplantation, Rega Institute, Immunity and Inflammation Research Group, Immunobiology Unit, KU Leuven, Leuven, Belgium
[e]KU Leuven Department of Microbiology, Immunology and Transplantation, Rega Institute, Laboratory of Virology and Chemotherapy, Translational Platform Virology and Chemotherapy, Leuven, Belgium
[f]KU Leuven Department of Imaging and Pathology, Translational Cell and Tissue Research, Leuven, Belgium

Summary

Background The live-attenuated yellow fever vaccine YF17D holds great promise as alternative viral vector vaccine platform, showcased by our previously presented potent severe acute respiratory syndrome coronavirus 2 (SARS-CoV-2) vaccine candidate YF-S0. Besides protection from SARS-CoV-2, YF-S0 also induced strong yellow fever virus (YFV)-specific immunity, suggestive for full dual activity. A vaccine concomitantly protecting from SARS-CoV-2 and YFV would be of great benefit for those living in YFV-endemic areas with limited access to current SARS-CoV-2 vaccines. However, for broader applicability, pre-existing vector immunity should not impact the potency of such YF17D-vectored vaccines.

Methods The immunogenicity and efficacy of YF-S0 against YFV and SARS-CoV-2 in the presence of strong pre-existing YFV immunity were evaluated in mouse and hamster challenge models.

Findings Here, we show that a single dose of YF-S0 is sufficient to induce strong humoral and cellular immunity against YFV as well as SARS-CoV-2 in mice and hamsters; resulting in full protection from vigorous YFV challenge in either model; in mice against lethal intracranial YF17D challenge, and in hamsters against viscerotropic infection and liver disease following challenge with highly pathogenic hamster-adapted YFV-Asibi strain. Importantly, strong pre-existing immunity against the YF17D vector did not interfere with subsequent YF-S0 vaccination in mice or hamsters; nor with protection conferred against SARS-CoV-2 strain B1.1.7 (Alpha variant) infection in hamsters.

Interpretation Our findings warrant the development of YF-S0 as dual SARS-CoV-2 and YFV vaccine. Contrary to other viral vaccine platforms, use of YF17D does not suffer from pre-existing vector immunity.

Funding Stated in the acknowledgments.

Keywords: SARS-CoV-2 vaccine; Yellow fever vaccine; Dual vaccine; Anti-vector immunity

eBioMedicine 2022;83: 104240
Published online xxx
https://doi.org/10.1016/j.ebiom.2022.104240

Introduction

Few human vaccines are considered as successful as the live-attenuated yellow fever YF17D legacy vaccine that was developed in the 1930s and is still used as essential tool to containing yellow fever virus (YFV) outbreaks. YF17D is exceptionally efficient in inducing vigorous

*Corresponding author.
E-mail address: kai.dallmeier@kuleuven.be (K. Dallmeier).

Research in context

Evidence before this study

Live-attenuated yellow fever vaccine YF17D is the basis for two licensed vaccines and other promising YF17D-based vaccine candidates, amongst others, Zika, HIV, Ebola, Lassa and malaria are under development. Generally, such derivatives inherit the excellent safety and immunogenicity profile from parental YF17D. We developed a YF17D-based SARS-CoV-2 vaccine candidate (YF-S0) that induced rapidly high level of neutralizing antibodies against both SARS-CoV-2 and YFV when tested in macaques, highlighting its potential as a dual-target vaccine. Generally, pre-existing flaviviruses immunity may interfere with subsequent infection or vaccination. However, though YF17D is a widely used vaccines as well as potent viral vector, the impact of pre-existing YFV immunity on such YF17D-derivatives remains largely unknown.

Added value of this study

In this study, we show that YF-S0 fully protects against lethal infection in a stringent intracranial YF17D challenge model in mice, and against vigorous challenge using hamster-adapted YFV Asibi in hamsters as relevant model that recapitulates yellow fever pathogenesis in humans. Such remarkable potency confirms superior efficacy of YF17D-vectored vaccines against not only the thus vectored target antigen but also YFV. When we evaluated the impact of pre-existing YFV immunity in these two animal models, there was no evidence that strong vector-specific immunity would hamper the immunogenicity or protective efficacy of YF-S0, neither in mice nor hamsters and much in contrast to other viral vector platforms currently used in vaccine development. Likewise, our data suggest that YF-S0 and other YF17D-derivatives can also successful be used in populations with a high yellow fever vaccine coverage, for instance in Africa and South America.

Implications of all the available evidence

This study strongly suggests that YF-S0 could serve as a dual vaccine against both SARS-CoV-2 and YFV. Moreover, unlike other viral vector vaccines, pre-existing YFV immunity has no notable impact on novel YF17D-derived vaccines, endorsing their use also in people that have been vaccinated before.

innate, long-lasting humoral and polyfunctional cell mediated immune (CMI) responses that possibly warrant life-long protection in most vaccinees.[1] This outstanding efficacy of YF17D is combined with a very favourable safety profile.[2]

YFV is a highly pathogenic mosquito-borne small RNA virus which may result in a up to 60% mortality in infected patients. Death is mainly caused by severe gastrointestinal bleeding, epileptic status, severe metabolic acidosis, necrohemorrhagic pancreatitis, and multi-organ failure after infection.[3] YFV is endemic in large parts of (sub)tropical Africa and Latin America, with more than one billion people living in areas of risk. Manufacturing in embryonated chicken eggs and need for a strict cold-chain for distribution make that classical YF17D vaccines are unable to keep up with the high global demand and YFV is estimated to still cause up to 60,000 fatalities annually.[2,4] After decades of relatively low epidemic activity, recently several large YFV outbreaks (Angola 2015-2016, DRC 2016, Brazil 2016-2019, Nigeria 2017) led to an unprecedented vaccine shortage and repeated depletion of the global YF17D emergency stockpile.[5] Furthermore, increasing global travel bares the risk of YFV being imported into regions where the virus is historically absent, such as the Asia Pacific region, that harbors both dense populations of competent vector mosquitos and billions of immunologically naïve people, raising serious concerns of massive future epidemics.[6,7] A more sustainable YF17D vaccine supply and novel vaccines against YFV are needed.[8]

Beyond its use as genuine YFV vaccine, YF17D serves a particularly potent vector platform for several licensed recombinant vaccines; ChimeriVax-JE/Imojev® against Japanese encephalitis and CYD-TDV/Dengvaxia® against dengue.[9] Other YF17D-based live vaccine candidates are under development, e.g. variants expressing foreign antigens from Lassa, Zika, or rabies virus, or therapeutic candidates for chronic hepatitis B.[10–13] Such YF17D derivatives generally inherit the excellent safety and immunogenicity features from parental YF17D.[9] However, little attention has been paid so far to the fact that the available YF17D backbone may, besides promoting the immunogenicity of the thus vectored new antigen, suffice to conjointly induce full protection from YFV infection as well; hence creating in fact dual target vaccines.[14,15] Likewise, the impact of pre-existing YFV immunity on the broader usability of YF17D as vaccine vector is limited to chimeric vaccines with their antigenic surface proteins swapped for those of other flaviviruses from distinct serogroups.[16] Notably, for other virus-vectored vaccines, such as adenovirus-based vaccines, pre-existing anti-vector immunity is known to strongly interfere, compromise or modify subsequent target antigen-specific immunogenicity.[17]

Recently, we engineered a live-attenuated YF17D vectored SARS-CoV-2 vaccine candidate (YF-S0), which expresses the non-cleavable stabilized prefusion form of the SARS-CoV-2 spike antigen as in-frame fusion within the YF17D-E/NS1 intergenic region. Two doses of YF-S0 given 7 days apart were shown to induce high levels of neutralizing antibodies (nAb) and strong antiviral CMI responses against both SARS-CoV-2, and resulted in full protection from SARS-CoV-2 infection in cynomolgus macaques and COVID-19-like lung pathology in a stringent hamster model. Moreover, in

hamsters a single high dose of YF-S0 was sufficient to confer 60% and 100% protection from vigorous challenge within 10 and 21 days post immunization, respectively.[18] YF-S0 safety was improved compared to parental YF17D, including in severely immune-compromised mice and hamsters, with limited biodistribution and shedding, and no mosquito transmission.[18,19] Importantly, in addition to strong SARS-CoV-2 immunity, YF-S0 consistently induced high levels of YFV-specific nAbs, correlating with protection from lethal intracranial YF17D challenge in type I interferon receptor-deficient (*Ifnar*$^{-/-}$) mice.[18,20] Such a dual activity of YF-S0 may serve as special asset in poorly developed regions, for instance of Africa, where vaccine supply for both YFV and COVID-19 remains challenging.[21]

Here, we further evaluate in particular the YFV-specific immunity induced by single-dose YF-S0 vaccination and show how it translates, alike original YF17D, into full protection against YFV challenge in both stringent mouse and hamster models. Finally, we demonstrate how full protection of hamsters from vigorous SARS-CoV-2 challenge can readily be achieved by single-dose YF-S0 immunization, including in animals with strong pre-existing YFV-specific immunity. This lack of interference with vector immunity is unparalleled and may be unique to the live-attenuated YF17D vector platform.

Methods

Cells

BHK-21J (baby hamster kidney fibroblasts) cells were kindly provided by Prof. P. Bredenbeek, LUMC, Leiden, The Netherlands and maintained in minimum essential medium (MEM, Gibco). Vero E6 (African green monkey kidney, ATCC CRL-1586) and HEK293T (human embryonic kidney cells, ATCC CRL-3216) cells were maintained in Dulbecco's modified Eagle medium (DMEM, Gibco). All growth media were supplemented with 10% fetal bovine serum (FBS, Hyclone), 2 mM L-glutamine (Gibco), 1% sodium bicarbonate (Gibco).

Viruses

All SARS-CoV-2 and hamster-adapted YFV Asibi related work was conducted in the high-containment BSL3 facilities of the KU Leuven Rega Institute (3CAPS) under licenses AMV 30112018 SBB 219 2018 0892 and AMV 23102017 SBB 219 2017 0589 according to institutional guidelines.

Vaccine viruses. The design and generation of live-attenuated YF-S0 vaccine virus has been described in great detail elsewhere.[18] YF17D virus, Stamaril® (lot G5400) (Sanofi-Pasteur) was passaged three times in Vero E6 cells before use. Medium used for production of virus stocks was identical to growth medium, yet containing only 2% fetal bovine serum. Virus titers were determined by plaque assay on BHK-21J cells, expressed as plaque forming units (PFU)/mL as described.[14]

Hamster-adapted YFV-Asibi virus construction and rescue. A hamster-adapted YFV-Asibi strain resembling clone molecular Ap7M as described by Klitting et al. was rescued using previously established PLLAV (Plasmid Launched Live Attenuated Virus) technology and standard recombinant DNA technology employing homologous recombination in yeast *S. cerevisiae*.[11,22,23] Briefly, the entire cDNA of YFV-Asibi clone Ap7M (Genbank accession number: MF926243) was divided into six fragments (A, B, C, D, E and F) averaging 2kb in size each with overlapping tails. The overall cloning strategy consisted of four steps (*i-iv*) and was based on the replacement of homologous YF17D sequences in pShuttle-YF17D and included the introduction of a selectable hygromycin-resistance cassette (derived from pAG26) as stuffer element (safety lock) in the thus assembled full-length viral cDNA; disrupting the YFV polyprotein ORF and hence facilitating work under BSL2 conditions.[11,24] (*i*) All six cDNA fragments were synthesized as gene blocks (IDT, Belgium), amplified by PCR and cloned into intermediary plasmids pJET (ThermoScientific) and pAG26 (EUROSCARF plasmid P30113).[24] The 3′-terminal fragment F was extended to attach a hepatitis delta virus ribozyme. Fragments A, B and C were fused by PCR and subcloned into pAG26. (*ii*) Fragment D and fused fragments EF were separately recombined (in yeast) into derivatives of pShuttle-YF17D (*i.e.* pShuttle-YF17D/Core-URA3 and pShuttle-YF17D/ENS1-URA3) replacing *URA3* markers (derived from pAG61, EUROSCARF plasmid P30112) in their respective Core and E/NS1 gene regions; yielding each a subgenomic (5' and 3' part) cDNA clone in a pShuttle backbone.[23,25] (*iii*) The resulting intermediary vectors (pD and pEF) were finally assembled with ABC in yeast to obtain non-functional, non-infectious but complete pABCDEF, *i.e.* a pShuttle-Asibi clone with the hygromycin resistance gene (safety lock) inserted in the XhoI site of the virus cDNA. All plasmids were validated by extensive restriction analysis and sequencing. (*iv*) Fully infectious YFV-Asibi cDNA was obtained by deleting the hygromycin resistance gene (via XhoI digest and religation) under BSL3 conditions. The thus obtained plasmid material was transfected into sub-confluent BHK-21J cells for virus rescue. Working virus stocks were obtained by passaging supernatants twice in BHK-21J cells. The genome of rescued hamster-adapted YFV-Asibi virus was confirmed by direct sequencing. Virus titers were determined by plaque assay on BHK-21J cells before.

SARS-CoV-2. SARS-CoV-2 virus B1.1.7 variant (hCoV-19/Belgium/rega-12211513/2020; EPI_ISL_791333, 2020-12-21), also known as variant of concern (VOC) Alpha, was selected as challenge strain due to its particularly high fitness and aggressive growth in hamsters.[26,27] Virus was grown on Vero E6 cells was used at passage 2, and median tissue culture infectious doses ($TCID_{50}$) were determined by titration using the Spearman-Kärber method. Strain identity and absence of furin site mutations in the virus stocks was confirmed by deep sequencing.[26]

Animals

Type I interferon receptor-deficient *Ifnar*$^{-/-}$ mice (*Mus musculus*) were bred in-house at the KU Leuven animal facility. Wild-type Syrian hamsters (*Mesocricetus auratus*) were purchased from Janvier Laboratories. Six to eight week-old male and female *Ifnar*$^{-/-}$ mice, and four week-old female hamsters were used throughout this study. All animals used were bred and housed (mice in groups of n=4-5; hamsters in pairs) under specific pathogen free (SPF) conditions in individually ventilated Isocages (Techniplast). Hamsters and mice were euthanized by intraperitoneal administration of 100 μL (mice) or 500 μL (hamsters) Dolethal (200 mg/mL sodium pentobarbital, Vétoquinol SA).[18,20,26]

Ethics

Housing conditions and experimental procedures were approved by the Ethical Committee of KU Leuven (license P015-2020), following Institutional Guidelines approved by the Federation of European Laboratory Animal Science Associations (FELASA).

YF-S0 immunization and intracranial challenge of mice with YF17D

For assessment of vaccine immunogenicity, *Ifnar*$^{-/-}$ mice were vaccinated intraperitoneally (i.p.) with a single 400 PFU dose of either YF-S0 or YF17D as positive control. Sham groups received a same volume of MEM containing 2% FBS (referred to as medium). I.p. administration of YF17D-based vaccine has previously been established by us as means for consistent immunization in mice (and hamsters), and to translate in a non-human primate model into immunogenicity and efficacy following vaccine delivery by the clinically more relevant subcutaneous route.[18] After three weeks, mice were bled and serum was separated for antibody detection by indirect immunofluorescence assay (IIFA) and serum neutralization test (SNT). Animals were then euthanized and spleens harvested for ELISpot and intracellular cytokine staining (ICS) (Figure 1b).

For assessment of vaccine efficacy, *Ifnar*$^{-/-}$ mice were vaccinated as before. Four weeks post-vaccination, mice were deeply anesthetized by intraperitoneal injection of a mixture of xylazine (16 mg kg^{-1}, XYL-M, V.M.D.), ketamine (40 mg kg^{-1}, Nimatek, EuroVet) and atropine (0.2 mg kg^{-1}, Sterop), and then intracranially injected with 30μl containing 3×10^3 PFU YF17D. In a first experiment (survival), thus challenged animals were monitored daily for signs of disease and weight change for the next four weeks. Sick mice were euthanized based on morbidity (hind limb paralysis, weakness and ruffled fur) or weight loss of more than 25%. Mice who died within four days post-challenge (caused by acute brain trauma) were excluded from further analysis. In a second experiment, thus challenged mice and healthy controls (without any vaccination nor challenge) were euthanized four days post-challenge, and organs (livers, spleens, kidneys and brains) were collected for analysis of resulting viral loads (quantification of virus RNA) and gene-expression profiling (Figure 1b).

YF-S0 Immunization and challenge infection of hamsters with hamster-adapted YFV Asibi virus

Hamsters were vaccinated i.p. with 10^4 PFU of either YF-S0 or YF17D as positive control at day 0, while sham groups received same volume of medium. Three weeks post-vaccination, animals were bled and challenged i.p. with 10^5 PFU of hamster-adapted YFV Asibi virus, a dose that has previously been shown to be 100% lethal in 3-weeks old hamsters.[22] Control groups did not receive any vaccination nor challenge. Hamsters were monitored daily for signs of disease and weight change and euthanized five days post-challenge to collect organs (livers, spleens and kidneys) and end sera. Liver samples were collected in formalin for histological assessment. Hamster-adapted YFV Asibi virus only causes mortality in 3-4 week-old young hamsters. Thus, those 7 week-old (upon challenge) hamsters were euthanized five days post-challenge, at reported peak of viral load in the liver and of inflammation[22] (Figure 2a).

Pre-immunization with YF17D and subsequent YF-S0 vaccination (boost) in mice

To assess the effect of pre-exiting vector immunity, *Ifnar*$^{-/-}$ mice were pre-immunized i.p. with 400 PFU of YF17D at day -14. Then at day 0 mice were bled (for detection of baseline antibody levels) and subsequently vaccinated i.p. with 400 PFU of YF-S0, or a same volume of medium (as "YF17D only" control). Another group of *Ifnar*$^{-/-}$ mice was sham vaccinated at day -14, bled at day 0 and then vaccinated i.p. with 400 PFU of YF-S0 (as "YF-S0 only" control) or with a same volume of medium (as sham control). Three weeks after last immunization (day 21), mice were bled for serology and their spleens harvested for ELISpot (Figure 3a).

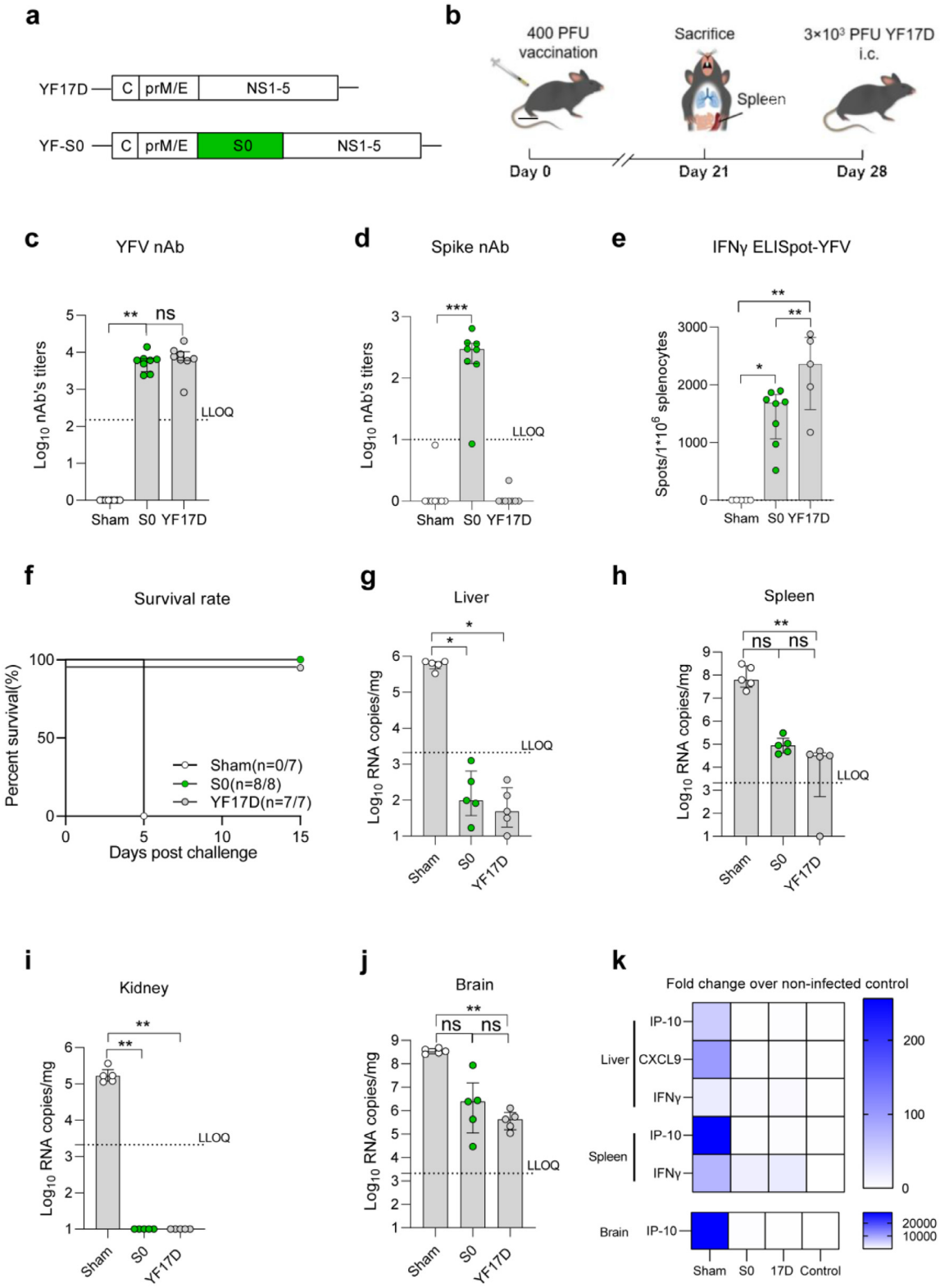

Figure 1. Immunogenicity and protective efficacy of single-dose YF-S0 vaccination in mice. (a) Schematic of parental YF17D and derived YF-S0. **(b)** *Ifnar*$^{-/-}$ mice were vaccinated with 400 PFU of either YF-S0 or YF17D, while sham group received same

Pre-immunization with YF17D, subsequent YF-S0 vaccination (boost) and challenge infection of hamsters with SARS-CoV-2 B1.1.7 variant

Hamsters were pre-immunized i.p with 10^4 PFU of YF17D or a same volume of medium at day -21 and boosted following a single-dose (at day 0) or two-dose (at day 0 and 7 separately) regimen using each 10^4 PFU of YF-S0, or a same volume of medium at day 0. Matched controls and sham groups received same volumes of medium. All hamsters were bled at day 0 and day 21 for serological analysis. At day 21, hamsters were anesthetized by i.p. injection of a mixture of xylazine (16 mg kg^{-1}, XYL-M, V.M.D.), ketamine (40 mg kg^{-1}, Nimatek, EuroVet) and atropine (0.2 mg kg^{-1}, Sterop) prior to challenge. Each hamster except hamsters from the control group was inoculated intranasally by gently adding a droplet of each 25 µl of virus stock containing in total 10^3 $TCID_{50}$ of SARS-CoV-2 B1.1.7 variant on each nostril. Hamsters were monitored daily for signs of disease (lethargy, heavy breathing or ruffled fur). Four days after challenge at peak of lung infection, animals were euthanized to collect end sera and lung tissue in MEM (for virus titration), or RNAlater (for gene-expression profiling)[26] (Figure 4a; S4a).

Indirect immunofluorescent assay (IIFA) for detection of total binding IgG, SARS-CoV-2 pseudotyped virus and YF17D virus serum neutralization test (SNT)

Quantitative detection of YFV-specific and SARS-CoV-2 spike-specific total binding IgG by means of indirect immunofluorescent assay (IIFA) and of neutralizing antibodies (nAb) has been described in great detail before.[18] In particular, SARS-CoV-2 nAb were determined using D614G spike-pseudotyped VSV-ΔG reporter viruses expressing GFP.[18,28[preprint]] YFV nAb were determined using mCherry-tagged YF17D reporter viruses.[18,28[preprint],29] All reagents were prepared and methods were performed accordingly.

ELISpot assay, intracellular cytokine staining (ICS) and flow cytometry

Assessment of YFV- and SARS-CoV-2-specific cell-mediated immunity (CMI) by ELISpot and Flow cytometry with ICS was performed as established and described before.[18,20] All peptides and reagents were prepared accordingly. The gating strategy used is outlined in Figure S1f.

RT-qPCR

RT-qPCR for lung homogenates was performed exactly as described in detail before.[18,26,30] For YFV viral RNA level qualification, RT-qPCR was performed using the ABI 7500 Fast Real-Time PCR System (Applied Biosystems) by using primers and probe derived from YFV non-structural gene 3 (Supplementary Table 3). For absolute YFV RNA quantification, standard curves were generated using five-fold dilutions of a cDNA plasmid template (plasmid pShuttle-YF17D) of known concentration. Based on repeated standard curves, the lower limit of qualification was established at 2,111 copies/mg brain tissue, corresponding to a C_t value of 33. C_t values above 33 were considered below the limit of qualification and represented as the square root of the lower limit of qualification.[20]

For gene-expression profiling, RT-qPCR was performed on a Light Cycler 96 platform (Roche) using the iTaq Universal Probes One-Step RT-qPCR Kit (BioRad) with primers and probes (Supplementary Table 3). The relative RNA fold-change was calculated with the $2^{-\Delta\Delta Cq}$ method using housekeeping gene Beta-actin (β-actin) for hamster samples and GAPDH for mouse samples for normalization.

End-point virus titrations

To quantify infectious SARS-CoV-2, end-point titrations were performed on confluent Vero E6 cells in 96-well plates. Lung tissues were homogenized using bead

volume of medium. **Humoral responses elicited by single YF-S0 vaccination in mice**. Titers of YFV-specific nAbs **(c)** and spike-specific nAbs **(d)** (n= 8 from two independent experiments) at day 21 post-vaccination. Dashed line represents lower limit of quantification (LLOQ). **Cellular responses elicited by single YF-S0 vaccination in mice**. *Ifnar*$^{-/-}$ mice were vaccinated with 400 PFU of either YF-S0 (n=8) or YF17D (n=5), while sham group (n=5) received same volume medium (from two independent experiments). Cellular responses were assessed by ELISpot of splenocytes harvested three weeks post-vaccination. **(e)** Spot counts for IFNγ producing cells per 10^6 splenocytes after stimulation with MHC-I restricted YFV NS3 peptide. **Protective efficacy of single YF-S0 vaccination against intracranial YF17D challenge in mice**. *Ifnar*$^{-/-}$ mice were vaccinated with 400 PFU of either YF-S0 or YF17D, while sham group received same volume medium (n=7, except for n=8 for YF-S0, from single experiment). Four weeks post-vaccination, animals were intracranially challenged with 3×10^3 PFU of YF17D. **(f)** Survival rate after challenge. Viral RNA copies were quantified by RT-qPCR in liver **(g)**, spleen **(h)**, kidney **(i)** and brain **(j)** four days post-challenge (n=5 per condition from single experiment). **(k)** Heat maps (generated with median) showing expression profile of selected cytokine genes in liver, spleen and brain of sham, YF17D and YF-S0 vaccinated *Ifnar*$^{-/-}$ mice four days after YF17D challenge (n=5 per condition from single experiment) (scale represents fold-change over healthy controls). RNA levels were determined by RT-qPCR on organ extracts, normalized for GAPDH mRNA levels and fold-changes over the median of uninfected controls were calculated using the $2^{(-\Delta\Delta Cq)}$ method. Data shown are median ± IQR. Data were analysed by Kruskal–Wallis test (one-way ANOVA) followed by Dunn's multiple comparison (ns = Not-Significant, $P > 0.05$, * $P < 0.05$, ** $P < 0.01$, *** $P < 0.001$).

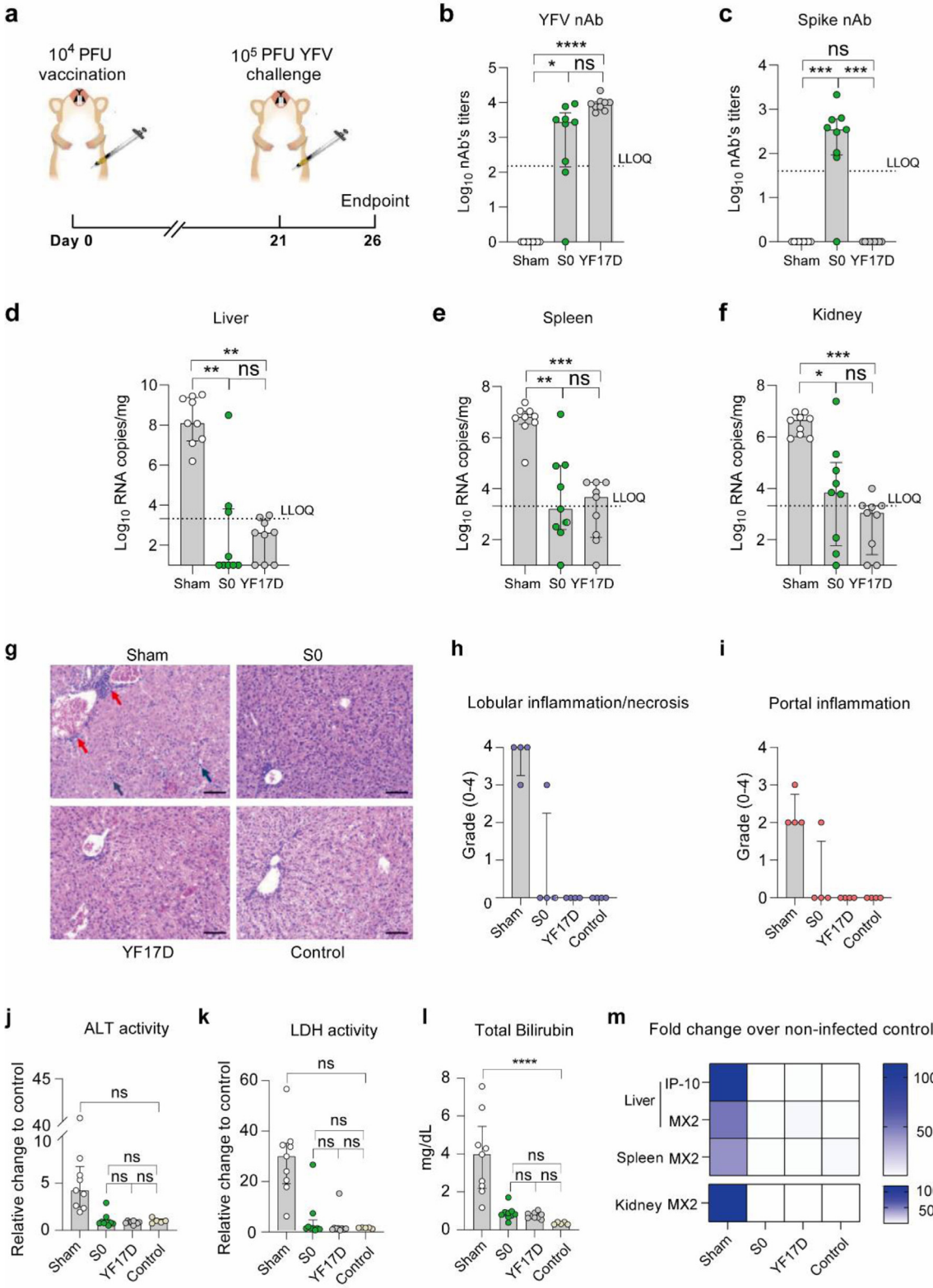

Figure 2. Immunogenicity and protective efficacy of single-dose YF-S0 vaccination in hamsters. (a) Four-week old hamsters were vaccinated with 10^4 PFU of either YF-S0 or YF17D, while sham group received same volume of medium. Three weeks post-

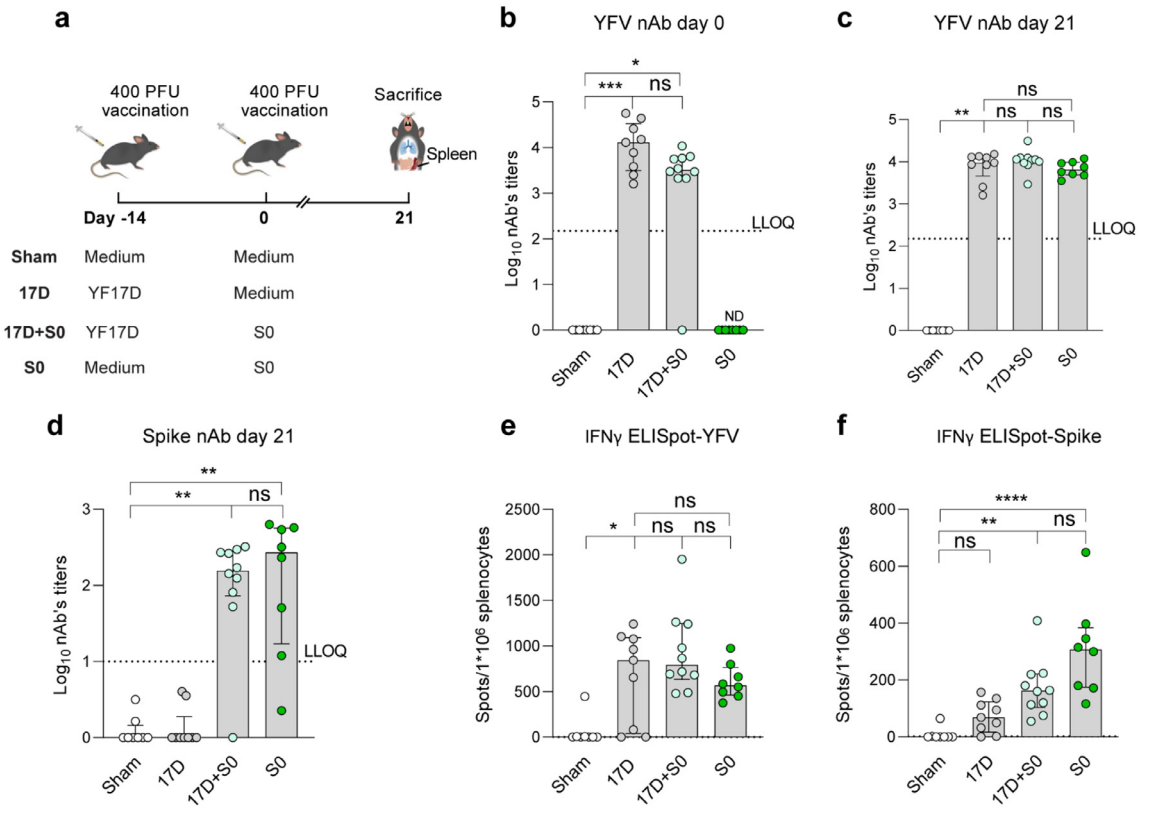

Figure 3. Impact of pre-existing YFV-specific immunity on immunogenicity of YF-S0 in mice. (a) *Ifnar*$^{-/-}$ mice were vaccinated with 400 PFU YF17D at day -14 and boosted with 400 PFU of YF-S0 (17D+S0; n =10) or same volume medium (YF17D; 2 = 9) at day 0. Another group of *Ifnar*$^{-/-}$ mice (YF-S0; n =8) received same volume medium at day -14 and 400 PFU YF-S0 at day 0, while sham group (n=7) received same volume of medium (from two independent experiments). YFV-specific nAbs titer at day 0 **(b)** (ND=not determined) and day 21 **(c)**; and spike-specific nAbs **(d)** titer at day 21. Dashed line represents lower limit of quantification (LLOQ). Cellular responses were assessed by ELISpot. Spot counts for IFNγ-producing cells per 10^6 splenocytes after stimulation with YFV NS4B peptide **(e)** or spike peptide **(f)** at day 21. Data shown are median ± IQR. Data were analysed by Kruskal–Wallis test (one-way ANOVA) followed by Dunn's multiple comparison (ns = Not-Significant, $P > 0.05$, * $P < 0.05$, ** $P < 0.01$, *** $P < 0.001$, **** $P < 0.0001$).

disruption (Precellys) in 250 μl MEM and centrifuged (10,000 rpm, 5 min, 4 °C) to pellet the cell debris. Viral titers were calculated by the Reed and Muench method and expressed as $TCID_{50}$ per mL tissue homogenate.[26]

Histology assessment for liver

For histological examination, liver was fixed in 4% paraformaldehyde and embedded in paraffin. Tissue sections (5 μm) were stained with hematoxylin and eosin,

vaccination, animals were intraperitoneally challenged with 10^5 PFU of hamster-adapted YFV Asibi (n=9 per condition from two independent experiments, except n=5 for uninfected controls from single experiment). **(b, c) Humoral responses induced by single YF-S0 vaccination in hamsters**. Titers of YFV-specific nAbs **(b)** and spike-specific nAbs **(c)** at day 21 post-vaccination. Dashed line represents lower limit of quantification (LLOQ). **(d-m) Protective efficacy of single YF-S0 vaccination against hamster-adapted YFV-Asibi challenge in hamsters**. Viral RNA copies were quantified by RT-qPCR in the liver **(d)**, spleen **(e)** and kidney **(f)** five days post-challenge. **(g)** Representative liver pathology in hamsters five days post-challenge. Hematoxylin-and-eosin-stained sections and histology grades of hamster liver. Lobular **(h)** (indicated by blue arrows) and portal **(i)** (indicated by red arrows) inflammation are graded from 0 to 3 (0, normal; 1, minimal; 2, moderate; 3, severe). Grade 4, additional hepatic necrosis in the presence of lobular inflammation. Scale bars, 200 μm. Relative activity of ALT **(j)** and LDH **(k)** to the median of healthy control, and total bilirubin levels **(l)** in hamster serum five days post-challenge. **(m)** Heat maps (generated with median) showing expression profile of selected cytokine genes in liver, spleen and kidney of sham, YF17D and YF-S0 vaccinated hamsters five days post hamster-adapted YFV-Asibi (scale represents fold-change over healthy controls). RNA levels were determined by RT-qPCR on organ extracts, normalized for β-actin mRNA levels and fold-changes over the median of uninfected controls were calculated using the $2^{(-\Delta\Delta Cq)}$ method. Data presented as median ± IQR. Data were analysed by Kruskal–Wallis test (one-way ANOVA) followed by Dunn's multiple comparison (ns = Not-Significant, $P > 0.05$, * $P < 0.05$, ** $P < 0.01$, *** $P < 0.001$).

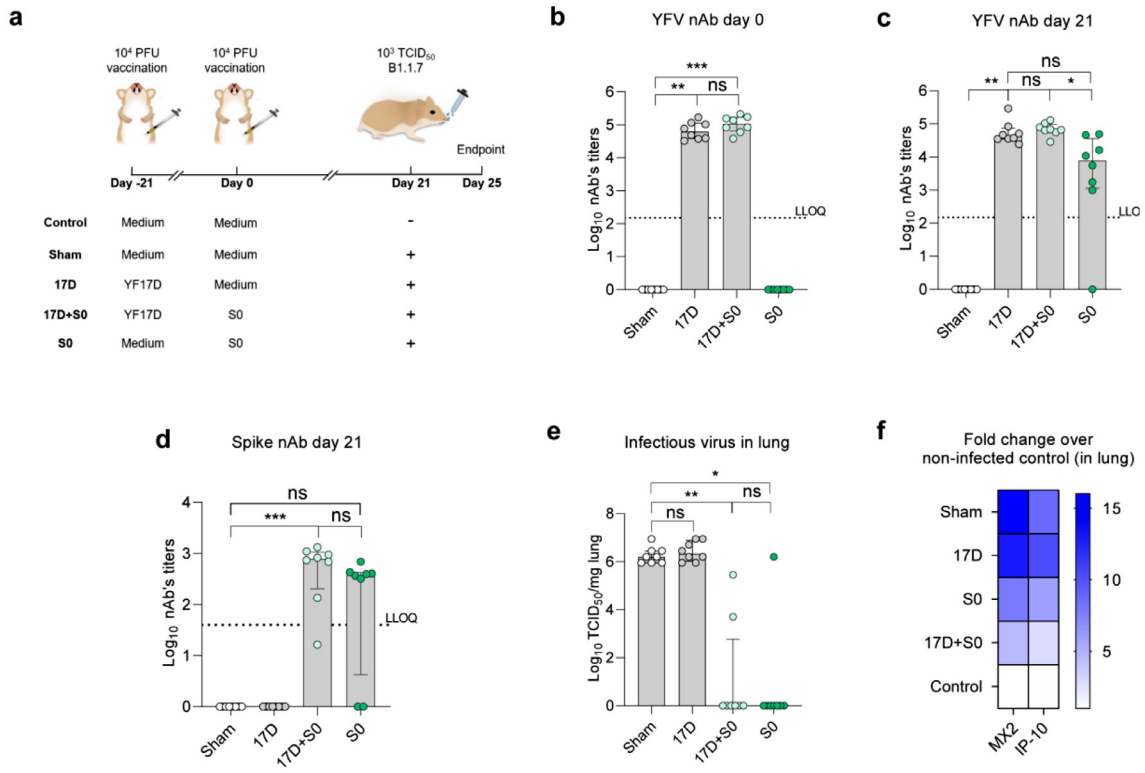

Figure 4. Impact of pre-existing YFV-specific immunity on immunogenicity of single-dose YF-S0 and protective efficacy against SARS-CoV-2 B1.1.7 variant challenge in hamsters. (a) Hamsters were vaccinated i.p with 10^4 PFU YF17D or same volume medium at day -21 and boosted with same volume medium or 10^4 PFU YF-S0 at day 0. Control and sham group received same volume of medium. All groups except control group were intranasally (i.n.) challenged with 10^3 $TCID_{50}$ of SARS-CoV-2 B1.1.7 variant at day 21 (n = 8 from two independent experiments). YFV-specific nAbs titer at day 0 **(b)** and day 21 **(c)**; and spike-specific nAbs titers at day 21 **(d)**. Dashed line represents lower limit of quantification (LLOQ). **(e)** Infectious viral loads in the lungs of hamsters four days after challenge are presented as $log_{10}TCID_{50}$ per mg lung tissue. **(f)** Heat map (generated with median) showing expression profile of mRNA levels of IP-10 and MX2 on lung extracts, normalized for β-actin mRNA levels. Fold-changes over the median of uninfected controls were calculated using the $2^{(-\Delta\Delta Cq)}$ method. Data shown are median ± IQR. Data were analysed by Kruskal–Wallis test (one-way ANOVA) followed by Dunn's multiple comparison (ns = Not-Significant, $P > 0.05$, * $P < 0.05$, ** $P < 0.01$, *** $P < 0.001$, **** $P < 0.0001$).

the extent and severity of the pathologic changes in each sample were evaluated observer-blinded by microscopic examination by a pathologist (T.R.) from the Department of Pathology, UZ Leuven. In liver sections, a grade was given by the degree of lobular/portal inflammation and hepatic necrosis: 0, normal; 1, minimal; 2, moderate; 3, severe. Score 4, additional hepatic necrosis in the presence of lobular inflammation.

Bilirubin, ALT and LDH assays

Total and direct bilirubin in serum sample were determined by using Bilirubin Assay Kit (cat. no. MAK126, Sigma-Aldrich, Belgium), according to the manufacturer's instructions. The activity of alanine aminotransferase (ALT) and Lactate dehydrogenase (LDH) were determined by using ALT Activity Assay kit (cat. no. MAK052, Sigma-Aldrich, Belgium) and LDH Activity Assay Kit (cat. no. MAK066, Sigma-Aldrich, Belgium), respectively. The data presented is the relative activity change as compared to the median value of healthy control group.

Statistical analysis

GraphPad Prism Version 9 (GraphPad Software, Inc.) was used for all statistical evaluations. The number of animals and independent experiments that were performed is indicated in the figure legends. Statistical significance was determined using non-parametric Mann-Whitney *U* test for pairwise comparisons or Kruskal-Wallis test with Dunn's post hoc test for multiple comparisons. Values were considered significantly different at *P* values of ≤0.05.

Role of funders
Funders had no roles in study design, data collection, data analyses, interpretation, or writing of report.

Results

Single dose YF-S0 vaccination elicits strong humoral and cellular responses against both YFV and SARS-CoV-2 spike, and fully protects against lethal intracranial YF17D challenge in mice.

Humoral responses, especially nAb are considered major correlates of protection from both YFV and SARS-CoV-2 infection.[1,31] Antibody responses were assessed in *Ifnar*$^{-/-}$ mice that are, in contrast to wild-type mice, readily susceptible to YF17D infection.[20] For that purpose, a single dose of as little as 400 plaque-forming units (PFU) of YF-S0 or YF17D (Figure 1a, b) was administered via the intraperitoneal (i.p.) route and sera sampled three weeks after vaccination. A similar yet two-dose protocol had earlier been shown to reflect robust immunization in a macaque model that employed a dose comparable to what is used clinically for YF17D administered via the subcutaneous route.[18]

Surprisingly, single YF-S0 vaccination elicited approximately equivalent levels of YFV-specific nAbs ($\log_{10}$-transformed geometric mean titres, $\log_{10}$ GMT 3.7, 95% CI 3.5−3.9) (Figure 1c) and total IgG ($\log_{10}$ GMT of 5.2, 95% CI 4.8−5.5) (Figure S1a) as YF17D vaccination ($\log_{10}$ GMT 3.8, 95% CI 3.5−4.1 for nAbs; $\log_{10}$ GMT 5.4, 95% CI 5.1−5.7 for IgG). Moreover, high levels of spike-specific nAbs ($\log_{10}$ GMT 2.3, 95% CI 1.8−2.8) (Figure 1d) and IgG ($\log_{10}$ GMT 3.3, 95% CI 3.1−3.5) (Figure S1b) were conjointly induced after a single low YF-S0 dose in mice.

To assess CMI responses, splenocytes were collected similarly three weeks after immunization (Figure 1b). Single YF-S0 vaccination resulted in marked YFV-specific T cell responses, as confirmed by a high number of spot-forming units in IFNγ ELISpot using a MHC-I restricted peptide derived from the YFV NS3 protein for re-stimulation (Figure 1e). Further profiling by intracellular straining (ICS) revealed the induction of YFV-specific CD4$^+$, CD8$^+$ and $\gamma\delta^+$ T cells producing IFNγ and TNFα after re-stimulation with a YFV NS4B peptide pool (Figure S1c), or likewise of CD8+ T cells probed by the NS3 peptide (Figure S1d). As expected, in YF-S0 vaccinated mice showed considerable CD8$^+$ and $\gamma\delta^+$ T cell responses to spike peptide (Figure S1e). A specific elevation of other markers such as IL-4 (Th2 polarization), IL-17A (Th17), or FoxP3 (regulatory T-cells) was not observed by the current ICS approach (not shown), yet has been confirmed earlier by qPCR.[18] In summary, single-dose YF-S0 vaccination induces robust humoral and Th1 CMI responses against both YFV and SARS-CoV-2 spike in mice.

To evaluate the protective efficacy of single YF-S0 against YFV infection, thus vaccinated *Ifnar*$^{-/-}$ mice were challenged with a lethal intracranial (i.c.) dose of 3×10^3 PFU of YF17D four weeks post-vaccination (Figure 1b). YF17D and sham-vaccinated animals served as positive and negative controls, respectively. I.c. challenge has been established as a stringent method to evaluate protection conferred by YF17D and YF17D-derived vaccines in mice.[11,15,20] All sham-immunized mice experienced acute weight loss and progressed rapidly to severe neurological disease with ruffled fur, hunched posture and hind limb paralysis, uniformly reaching human endpoint as early as five days post infection (dpi) (Figure 1f), whereas full protection was conferred in mice vaccinated with either YF-S0 or YF17D, as confirmed by the absence of any signs of disease, rapid recovery and weight gain (Figure S1g). High level of viral RNA loads was detected in liver (with mean viral RNA loads $10^{5.7}$ copies/mg tissue), spleen ($10^{7.9}$ copies/mg), kidney ($10^{5.2}$ copies/mg), and brain ($10^{8.5}$ copies/mg) of sham-immunized controls. In contrast, in YF-S0 vaccinated mice 4 dpi no viral RNA was detectable anymore in livers and kidneys, and viral RNA loads were significantly reduced in their brains and spleens; comparable to original YF17D vaccination (Figure 1g-j). Also, single YF-S0 resulted, like YF17D vaccination, in an almost complete normalization of cytokine expression profiles serving as a sensitive marker of viscerotropic and neurotropic YFV disease; especially in the liver, regarding IP-10 (as a marker for liver disease initiation and progression), CXCL9 (liver damage) and IFNγ (Figure 1k; S1h).[32,33] Similarly, IP-10 and IFNγ showed normal expression in the spleens and brains of YF-S0 and YF17D vaccinated mice equaling healthy controls; hence markedly lower than in sham-immunized mice (Figure 1k; S1h). Together these data indicate that single YF-S0 vaccination provides full protection against YF17D i.c. challenge as well as YFV-induced inflammatory damage to the liver and other relevant target organs in mice, comparable to original YF17D.[18]

Single YF-S0 vaccination induces robust humoral responses against both YFV and spike, and provides full protection against a YFV-Asibi challenge and YFV-induced viscerotropic disease in hamsters.

Hamster-adapted YFV-Asibi strain causes viscerotropic disease in adult hamsters replicating key clinical features of genuine YFV infection in humans; likewise, full lethality is observed only in young (3-4 week-old) hamsters.[22,34] To confirm the protective efficacy of YF-S0 against genuine YFV infection, four week-old hamsters were immunized i.p. with 10^4 PFU of either YF-S0 or YF17D, and challenged three weeks post-vaccination with a 10^5 PFU i.p. dose of hamster-adapted YFV-Asibi virus (Figure 2a) that had been rescued using previously established PLLAV technology.[11,19] A single dose of YF-S0 induced consistently high levels of YFV-specific nAbs ($\log_{10}$ GMT 2.9, 95% CI 1.9−3.9) (Figure 2b) and IgG ($\log_{10}$ GMT 3.8, 95% CI 2.6−4.9) (Figure S2a)

in 8 out of 9 vaccinated hamsters (primary vaccine failure in 1/9); comparable to original YF17D regarding IgG and somewhat lower for nAbs (YF17D: log_{10} GMT 4.2, 95% CI 4.0−4.4 and log_{10} GMT 4.0, 95% CI 3.8−4.1, respectively) (Figure 2b; S2a). Notably, in either case, nAbs levels largely exceeded nAb titers >1:40 considered to correlate with protection in the hamster model.[35] Consistent with YF-S0 vaccination in *Ifnar*$^{-/-}$ mice and previously published data,[18,28[preprint]] strong spike-specific nAbs responses (log_{10} GMT 2.3, 95% CI 1.5−3.0) (Figure 2c) and IgG (log_{10} GMT 2.8, 95% CI 1.9−3.6) (Figure S2b) were conjointly induced.

After challenge, hamsters vaccinated with either YF17D or YF-S0 remained healthy, while sham-immunized animals suffered from clear signs of severe YFV-induced disease such as desiccation, lethargy, growth retardation and weight loss, and had to be euthanized as early as 5 dpi (Figure S2c). Accordingly at necropsy, livers of sham-immunized hamsters appeared macroscopically paler and softer than normal livers of YF-S0 and YF17D vaccinated hamsters. Further, high viral RNA loads were detected in liver (mean viral RNA load $10^{8.2}$ copies/mg tissue), spleen ($10^{6.0}$ copies/mg) and kidney ($10^{6.4}$ copies/mg) of all sham-immunized hamsters (Figure 2d-f). By contrast, with exception of the one animal that had not seroconverted (Figure 2b-c), viral RNA remained undetectable in the livers of the majority (6/9) of YF-S0 vaccinated hamsters, and showed a marked reduction in spleens and kidneys similar to YF17D vaccinated animals. Moreover, compared to a completely normal liver histology in YF-S0 or YF17D immunized animals, livers of sham-immunized hamsters showed significant pathological changes (Figure 2g), including severe lobular inflammation, portal inflammation, and severe hepatic necrosis, consistent with the high viral loads detected in the liver (Figure 2h, i).

Liver function and damage were measured by serum alanine transaminase (ALT) and lactate dehydrogenase (LDH), and total and direct bilirubin levels.[34] ALT (liver injury and hepatic necrosis; Figure 2j) and LDH (tissue damage and toxicity; Figure 2k) activity was markedly increased following YFV-Asibi challenge in sham-immunized hamsters 5 dpi, whereas no significant elevation was detected in YF-S0 or YF17D immunized hamsters over healthy controls. Similarly, significantly elevated levels of bilirubin (total: 3.8 mg/dL, 95% CI 2.3−5.5 mg/dL; direct: 1.9 mg/dL, 95% CI 1.3−2.5mg/dL; geometric means) were detected in sham-immunized hamsters, indicative for icteric malfunction of the liver. In contrast, bilirubin levels in YF-S0 and YF17D immunized hamsters were in the normal range (reference: 0.1−0.9 mg/dL),[34] though slightly increased compared to healthy controls (Figure 3l; S2d).

Finally, immunization with either YF-S0 or YF17D resulted in a nearly complete normalization of intrahepatic IP-10 chemokine expression (Figure 2m; S2e). In addition, these hamsters also showed no systemic MX2 expression anymore (Figure 2m; S2e), an IFN-stimulated gene triggered by virus infection.[18,30] Collectively, these results indicate that single-dose YF-S0 vaccination provides full protection against YFV challenge and virus-induced viscerotropic disease in hamsters, comparable to original YF17D.

Pre-existing YFV-specific immunity has no notable impact on YF-S0 induced SARS-CoV-2 specific immunity in mice

Pre-existing anti-vector immunity is of general concern regarding the wide application of viral vector vaccines.[36] Previous flaviviruses exposure has been reported to influence the outcomes of subsequent heterologous flavivirus infections and vaccination.[37−40] Given (*i*) that people living in YFV-endemic areas may have ideally received yellow fever vaccination before, and (*ii*) considering the exceptional durability of YF17D-induced immunity in humans,[1] it is essential to determine to what extent immunogenicity and protective efficacy of YF-S0 will be impacted by pre-existing YFV immunity.

To assess the role pre-existing vector immunity may play, *Ifnar*$^{-/-}$ mice vaccinated with 400 PFU of YF17D (at day -14) were subsequently re-vaccinated (boosted) with 400 PFU of YF-S0 or medium two weeks post prime immunization (day 0; Figure 3a). As reported earlier, YF17D-induced humoral responses reach a plateau around two weeks post-vaccination in *Ifnar*$^{-/-}$ mice.[20] As expected, high levels of YFV-specific antibodies (nAbs: log_{10} GMT >3.2) (Figure 3b, Table 1a) were hence induced in all YF17D-immunized mice at day 0, whereas YF-S0 vaccination boosted these pre-established YFV-specific antibodies by about 6-fold (YF17D +S0; Figure 3c). However, no significant differences were observed in YFV-specific T cell responses among different vaccinated groups, as confirmed by IFNγ ELISpot (Figure 3e, Table 1b). Importantly, such strong YFV-specific immunity (Figure 3b) had no impact ($p>0.5$; Kruskal−Wallis test) on YF-S0 induced spike-specific nAbs (Figure 3d) nor IgG (Figure S3a) responses in mice (17D+S0 group; Table 1a). Furthermore, as demonstrated by IFNγ ELISpot (Figure 3f, Table 1b), also obvious spike-specific T cell responses were induced in the presence of this strong pre-existing YFV-specific immunity (17D+S0 group), albeit possibly to some lesser extent than to naïve mice solely vaccinated with YF-S0 (S0 group). In summary, strong pre-existing YFV vector-specific immunity has no major impact on the immunogenicity live YF17D-vectored YF-S0 in mice.

a

	YFV-nAbs day 0	YFV-nAbs day 21	Spike-bAbs day 21	Spike-nAbs day 21
Sham	0.00 ± 0.00	0.00 ± 0.00	0.00 ± 0.00	0.00 ± 0.00
17D	4.02 ± 0.42	3.89 ± 0.26	0.00 ± 0.00	0.00 ± 0.00
17D + S0	3.25 ± 0.83	4.02 ± 0.18	2.55 ± 0.69	1.99 ± 0.53
S0	ND	3.82 ± 0.15	2.95 ± 1.07	2.04 ± 0.76

b

IFNγ ELIspot day 21	YFV NS4B peptide	Spike peptide pool
Sham	58 ± 131	8 ± 19
17D	662 ± 388	72 ± 43
17D + S0	935 ± 322	171 ± 71
S0	611 ± 164	309 ± 140

***Table 1*: a. Mean and 95% confidence interval (Mean ± 95% CI) value of Log_{10}-transformed reciprocal titers for YFV-specific nAbs (in Figure 3b, 3c), spike-specific nAbs (in Figure 3d) and bAbs (in Figure S3a) titers. The lower limit of quantification (LLOQ) of SNT assay to determine YFV- and spike-specific nAbs titer was 2.2 Log_{10} (≥1:150) and 1 Log_{10} (≥1:10), respectively; whereas the lower limit of detection (LLOD) of IIFA assay to determine the spike-specific bAbs titer was 1.1 Log_{10} (≥1:12.5). b. mean ± 95% CI value of spot counts for IFNγ-producing cells per 10^6 splenocytes after stimulation with either YFV NS4B peptide (in Figure 3e) or spike peptide pool (in Figure 3f).**

Pre-existing YFV-specific immunity has no notable impact on YF-S0 induced SARS-CoV-2 specific humoral responses nor protective efficacy against SARS-CoV-2 infection in hamsters

Like other currently licensed COVID-19 vaccines, YF-S0 expresses a prefusion-stabilized SARS-CoV-2 spike protein of prototypic WA1 strain (spike from the 2019 variant Wuhan-Hu-1).[31] An updated version of YF-S0 expressing an adapted spike sequence to cover emerging SARS-CoV-2 variants of concern (VOC) is under development (YF-S0*; Sharma et al. BioRxiv).[28] Cosmopolitan SARS-CoV-2 lineage B.1.1.7 (VOC Alpha) dominated the pandemic in the first half of 2021 and was shown to cause particularly aggressive infections in the hamster model.[26,27]

To evaluate the impact of YF17D vector-specific immunity on the immunogenicity and protective efficacy of YF-S0 against aggressive B1.1.17 variant infection, hamsters were first immunized against YFV using 10^4 PFU YF17D (at day -21) prior to subsequent vaccination against SARS-CoV-2 following either a single (17D +S0) (day 0; 10^4 PFU) (Figure 4a) or two-dose (17D +2S0) (day 0 and 7; 10^4 PFU) (Figure S4a) regimen of YF-S0. Animals were subsequently challenged intranasally with 10^3 $TCID_{50}$ of SARS-CoV-2 B1.1.7 variant at day 21.

By day 0 prior to YF-S0 vaccination, consistently high levels of YFV-specific nAbs (log_{10} GMT > 4.8) were present in all YF17D-immunized hamsters (Figure 4b, Table 2). As expected, pre-existing YFV-specific antibody responses (as of day 0) were boosted by either a single- (Figure 4b, c) or two-dose (Figure S4b, c) YF-S0 vaccination by day 21 (Table 2). Importantly, spike-specific nAbs (log_{10} GMT > 1.9) were elicited in all vaccinated hamsters with or without pre-existing YFV-specific nAbs (Table 2). No significant differences were observed between the single YF-S0 vaccination group (S0; log_{10} GMT 2.0, 95% CI 0.9–3.0) and the 17D+S0 group (log_{10} GMT 2.6, 95% CI 2.1–3.2) (Figure 4d); nor between the dual YF-S0 vaccination group (2S0; log_{10} GMT 2.2, 95% CI 1.1–3.1) and the 17D+2S0 group (log_{10} GMT 2.3, 95% CI 2.0–2.6) (Figure S4d, Table 2). These data indicate that strong pre-existing YF17D vector immunity has no major impact on the mounting of vigorous humoral immune responses induced by either a single- or two-dose YF-S0 vaccination in hamsters, fully corroborating immunogenicity data obtained in mice.

Thus treated animals were subsequently infected with B1.1.7 virus via the nasal route. Resulting virus replication in the lower respiratory tract was monitored by virus titration of lung homogenates 4 dpi. As established before,[18,28[preprint]] high infectious virus loads (mean 6.2 log_{10} $TCID_{50}$/mg) were detected in the lungs of sham- or YF17D-immunized hamsters. By contrast no infectious virus was detected in most (7/8) single YF-S0-immunzied hamsters (Figure 4e), and infectious virus was absent from all (8/8) of the two-dose YF-S0-immunized hamsters (Figure S4e). These results confirm that besides dual- (Sharma et al. BioRxiv) also single-dose YF-S0 vaccination can provide protection against B1.1.7 variant infection in hamsters.[28[preprint]] In a few animals protection against B1.1.7 variant infection was noticed even in the absence of detectable spike-specific nAbs (Figure 4d; S4d, S4g), suggesting that except nAbs, also other immune components contribute to protection against SARS-CoV-2.[31]

	YFV-nAbs day 0	YFV-nAbs day 21	Spike-nAbs day 21	$TCID_{50}$/mg
Sham	0.00 ± 0.00	0.00 ± 0.00	0.00 ± 0.00	6.26 ± 0.29
17D	4.82 ± 0.22	4.73 ± 0.28	0.00 ± 0.00	6.32 ± 0.34
S0	0.00 ± 0.00	3.45 ± 1.27	1.97 ± 1.02	0.77 ± 1.83
17D + S0	5.00 ± 0.21	4.84 ± 0.16	2.64 ± 0.54	1.14 ± 1.81
2S0	0.00 ± 0.00	4.21 ± 0.48	2.22 ± 0.91	0.00 ± 0.00
17D + 2S0	4.80 ± 0.12	5.04 ± 0.23	2.29 ± 0.27	0.00 ± 0.00

***Table 2*: Mean ± 95% CI value of Log_{10}-transformed reciprocal titers for YFV-specific nAbs (in Figure 4b-c; S4b-c), spike-specific nAbs (in Figure 4d; S4d) titers and $TCID_{50}$/mg lung tissue (in Figure 4e; S4e). The lower limit of quantification (LLOQ) of SNT assay to determine YFV-specific and spike-specific nAbs titer was 2.2 Log10 (≥1:150) and 1.6 Log10 (≥1:40), respectively.**

Importantly, also when animals were vaccinated in the presence of strong YFV-specific nAbs, most hamsters (6/8) in the 17D+S0 group and all hamsters (8/8) in the 17D+2S0 group were protected from B1.1.7 infection. This was demonstrated by the absence of any detectable infectious virus in their lungs 4 dpi (Figure 4e; S4e). High level of protection is further supported by a marked reduction in the expression of IP-10 and MX2 (serving as markers for inflammation and lung pathology)[18,26,30] in the lungs of YF-S0 vaccinated hamsters compared to sham- and YF17D-immunized controls (Figure 4f; S4f). In summary, these results suggest that strong pre-existing YFV immunity has no major impact on protection against stringent SARS-CoV-2 infection challenge conferred by either single- or two-dose YF-S0 vaccination. Such overruling of vector-specific immunity by live YF17D-vectored vaccines can be expected to be independent of the inserted foreign antigen.

Discussion

More than 30 vaccines and vaccine candidates have been authorized for (conditional) use in humans, significantly contributing to the control of the ongoing COVID-19 pandemic. However, current first-generation COVID-19 vaccines are unlikely to hit all real-world challenges linked to global immunization. Certainly, the world will benefit from an expanded vaccine portfolio that allows countries to select most suitable vaccines considering the specific needs of their healthcare system, population structure, cold chain capacity and of manufacturing cost, amongst many other critical factors.[41] Particularly, readily affordable and accessible, and likewise safe and potent COVID-19 vaccines are needed to control the pandemic at global scale, including in regions for instance of Africa with underdeveloped healthcare systems, where vaccine supply generally remains challenging in light of an already heavy burden of (re-)emerging infectious diseases.[42,43] Additionally, the COVID-19 crisis has disrupted production and access to other essential vaccines and on-going vaccination campaigns, including yellow fever immunization, increasing the disease burden and risk of future outbreaks concomitant with SARS-CoV-2.[21,44] A dual-target vaccine like YF-S0 or its variant-proof updated version YF-S0* (Sharma et al. BioRxiv)[28] might hence be of extra benefit for those regions of African and South America in which also YFV is endemic.

Previously, we demonstrated that YF-S0, next to being well tolerated, highly immunogenic and effective against SARS-CoV-2 prototypic WA1 strain, led in cynomolgus macaques also to the rapid induction of YFV-specific nAbs that were excessively higher than what is required to protect from lethal YFV infection.[1,18] In full support of these data, we now show that a single dose of YF-S0 was sufficient to elicit high nAbs and IgG levels against both YFV and spike in mice (Figure 1c-d; S1a-b) and hamsters (Figure 2b-c; S2a-b); as well as robust and polyfunctional CMI against both YFV (Figure 1e; S1c-d; 3e) and spike (Figure S1e; 3f) as demonstrated in mice. Moreover, this single-dose YF-S0 vaccination fully protects against lethal intracranial YF17D challenge and YFV-induced organ damage in a stringent *Ifnar*$^{-/-}$ mouse model (Figure 1f-k; S1f).[11,14,15,20] Hamster represents a relevant small animal model, which reproduces key symptoms of human YFV infection and viscerotropic disease after hamster-adapted YFV Asibi infection.[22,34] Remarkably, our results indicate that single-dose YF-S0 vaccination provides full protection against vigorous YFV challenge (Figure 2d-i; S2c) as well as YFV-induced viscerotropic disease (Figure 2j-m; S2d), comparable to YF17D immunization. Collectively, YF-S0 also represents a potent YFV vaccine candidate. Formal assessment of clinical efficacy in human clinical trials for such a dual target product may be challenging. Nevertheless, the excellent YFV antibody responses concomitantly induced by YF-S0 vaccination may suffice as correlate of protection.[1,2] Likewise, with growing insight into SARS-CoV-2 immunity, also future COVID-19 vaccines may get licensed solely through demonstration of protective immune responses,[45] possibly based on serological markers such as anti-RBD IgG and neutralizing titers.[46]

A general issue regarding viral vector vaccines concerns their sensitivity to pre-existing anti-vector immunity.[17,36,47] Anti-vector immunity has shown profound impact particularly on non-replicating viral vector vaccines, such as replication-defective herpes simplex

virus 1 (HSV-1)-based and various adenovirus (Ad)-based recombinant vaccines (including multiple serotypes: Ad5, Ad11, Ad35, and chimpanzee Ad) in both mice and rhesus monkeys, as well as in phase I human clinical trials.[48–54] In contrast, on live replication-competent viral vectors pre-existing anti-vector immunity seems to have a limited impact, as anti-measles immunity had only a minor impact on the performance of recombinant measles virus-based vaccines in mice, macaques or humans.[55–58] Pre-existing flavivirus immunity could affect the infection outcomes and immunogenicity of subsequent flavivirus infection or vaccination.[37–39] Most studies have focused on the interference between dengue and Zika viruses as closely antigenically related and potentially prone to antibody-dependent enhancement (ADE) of infection.[37,38] However, despite being a widely used human vaccine and desirable viral vector, investigations on the impact of pre-existing YFV-specific immunity are limited.[1,9] Interestingly, in phase 3 human trials of YF17D-based dengue vaccine CYD-TDV/Dengvaxia®, subjects with prior flaviviruses infections demonstrated rather an improved than compromised immunogenicity compared to immunologically flaviviruses naïve recipients.[59,60]

Here, by trialling our YF-S0 vaccine candidate first in mice and then in hamsters, we demonstrate that at least under the preclinical conditions tested, strong pre-existing YFV-specific immunity has no major impact on YF-S0 induced humoral responses (Figure 3d; S3a; 4d; S4d). Some (non-significant) reduction in CMI (Figure 3f) observed in mice is consistent with the relatively higher impact of pre-existing anti-vector immunity on subsequent cellular immunity, further depending on the animal model used.[37,53,61] Importantly, we clearly demonstrate that pre-existing YFV-specific immunity does not lead to a reduction in the efficacy of YF-S0 to protect against SARS-CoV-2 B1.1.7 variant in hamsters (Figure 4e; S4e), neither after a single- nor two-dose vaccination. Of note, several YF17D-derived vaccine candidates primarily targeting African populations, including those against dengue, human immunodeficiency virus (HIV), malaria, Ebola and Lassa, are currently being tested.[9,11,12,16] Our results strongly suggest that it might be feasible to use YF-S0 and other YF17D derivatives in those YFV seropositive populations, either in a single-does or two-dose regiment.

Taken together, YF-S0 represents as a potent dual vaccine candidate against both SARS-CoV-2 and YFV infection, possibly feasible as single-dose vaccination. Such a dual vaccine would be of benefit for (*i*) containing current COVID-19 pandemic; (*ii*) alleviating the burden of YF17D vaccine shortage; (*iii*) contributing to the WHO Eliminate Yellow Fever Epidemics (EYE) programme; and (*iv*) at once precluding potential YFV outbreaks in areas such as in Asia-Pacific region from which the virus is historically absent while actually implementing a COVID-19 immunization program. More in general, both dual protection and maintaining of vaccine efficacy in subjects with strong pre-existing vector immunity are unique and should translate to other vaccines built on the same the live-attenuated YF17D vector platform.

Contributors

J.M. and K.D. conceptualized and designed the experiments. J.M. performed animals experimentation, data generation and analysis, curation, original manuscript draft; J.M, H.J.T. and K.D. verified the underlying data; M.B.Y. and S.J. developed and provided hamster-adapted YFV Asibi virus; J.M. and B.M.D. performed ELISpot assay and flow cytometry with intracellular staining; L.S.F. provided vaccine constructs; D.V.L., T. V. and H.J.T. performed serological analysis; B.W. and T.R. conducted the histological analysis; M.P.A.J performed intracranial injection in mice; J.N., K.D. and O. Q. supervised projects and acquired funding; J.M. draft manuscript; P.M. and O.Q. provided advice on data interpretation and critical edits to the text; J.M, H.J.T. and K.D. finalized manuscript with help of all co-authors; all authors read and approved the final manuscript.

Data sharing statement

The authors declare that all data supporting the findings of this study are presented in this manuscript and are available from the corresponding author upon request.

Declaration of interests

The authors have nothing to disclose.

Acknowledgements

We thank the staff of the Rega animalium for strong support. We thank Xin Zhang, Robbert Boudewijns and Viktor Lemmens for help with virus titrations, analysing of tissue samples by ELISA and qPCR and preparation of vaccine virus stocks. We finally thank Jasmine Paulissen, and Nathalie Thys (TPVC) for serology assessment. Current work was supported by the Flemish Research Foundation (FWO) emergency COVID-19 fund (G0G4820N) and the FWO Excellence of Science (EOS) program (No. 30981113; VirEOS project and No. 40007527; VirEOS2), the European Union's Horizon 2020 research and innovation program (No. 733176; RABYD-VAX consortium), KU Leuven Internal Funds (C24/17/061 and C24M/19/006), the KU Leuven/UZ Leuven Covid-19 Fund (COVAX-PREC project) and European Health Emergency Preparedness and Response Authority (HERA; HE OMICRON BEL project). J.M. acknowledges grant support from the Chinese

Scholarship Council (CSC; No. 201706760059) and K. D. from KU Leuven Internal Funds (C3/19/057; Lab of Excellence).

Supplementary materials

Supplementary material associated with this article can be found in the online version at doi:10.1016/j.ebiom.2022.104240.

References

1 Pulendran B. Learning immunology from the yellow fever vaccine: Innate immunity to systems vaccinology. *Nat Rev Immunol*. 2009;9:741–747.
2 Staples JE, Barrett ADT, Wilder-Smith A, Hombach J. Review of data and knowledge gaps regarding yellow fever vaccine-induced immunity and duration of protection. *npj Vaccines*. 2020;5:1–7.
3 Ho YL, Joelsons D, Leite GFC, et al. Severe yellow fever in Brazil: Clinical characteristics and management. *J Travel Med*. 2019;26:1–7.
4 Shearer FM, Moyes CL, Pigott DM, et al. Global yellow fever vaccination coverage from 1970 to 2016: an adjusted retrospective analysis. *Lancet Infect Dis*. 2017;17:1209–1217.
5 Kraemer MUG, Faria NR, Reiner RC, et al. Spread of yellow fever virus outbreak in angola and the democratic republic of the Congo 2015–16: a modelling study. *Lancet Infect Dis*. 2017;17:330–338.
6 Lataillade L de G de, Vazeille M, Obadia T, et al. Risk of yellow fever virus transmission in the Asia-Pacific region. *Nat Commun*. 2020;11:1–10.
7 Cracknell Daniels B, Gaythorpe K, Imai N, Dorigatti I. Yellow fever in Asia-a risk analysis. *J Travel Med*. 2021;28:1–12.
8 Hansen CA, Barrett ADT. The present and future of yellow fever vaccines. *Pharmaceuticals*. 2021;14:1–26.
9 Bonaldo MC, Sequeira PC, Galler R. The yellow fever 17D virus as a platform for new live attenuated vaccines. *Hum Vaccines Immunother*. 2014;10:1256–1265.
10 Rupprecht CE, Abela-Ridder B, Abila R, et al. Towards rabies elimination in the Asia-pacific region: from theory to practice. *Biologicals*. 2020;64:83–95.
11 Kum DB, Mishra N, Boudewijns R, et al. A yellow fever–Zika chimeric virus vaccine candidate protects against Zika infection and congenital malformations in mice. *npj Vaccines*. 2018;3:1–14.
12 Jiang X, Dalebout TJ, Bredenbeek PJ, et al. Yellow fever 17D-vectored vaccines expressing Lassa virus GP1 and GP2 glycoproteins provide protection against fatal disease in guinea pigs. *Vaccine*. 2011;29:1248–1257.
13 Boudewijns R, Ma J, Neyts J, Dallmeier K. A novel therapeutic HBV vaccine candidate induces strong polyfunctional cytotoxic T cell responses in mice. *JHEP Reports*. 2021;3:100295.
14 Mishra N, Boudewijns R, Schmid MA, et al. A chimeric Japanese encephalitis vaccine protects against lethal yellow fever virus infection without inducing neutralizing antibodies. *MBio*. 2020;11:02494-19.
15 Kum DB, Boudewijns R, Ma J, et al. A chimeric yellow fever-Zika virus vaccine candidate fully protects against yellow fever virus infection in mice. *Emerg Microbes Infect*. 2020;9:520–533.
16 Guirakhoo F, Kitchener S, Morrison D, et al. Live attenuated chimeric yellow fever dengue type 2 (ChimeriVax-DEN2) vaccine: Phase I clinical trial for safety and immunogenicity: effect of yellow fever pre-immunity in induction of cross neutralizing antibody responses to all 4 dengue serotypes. *Hum Vaccin*. 2006;2:60–67.
17 Lasaro MO, Ertl HCJ. New insights on adenovirus as vaccine vectors. *Mol Ther*. 2009;17:1333–1339.
18 Sanchez-Felipe L, Vercruysse T, Sharma S, et al. A single-dose live-attenuated YF17D-vectored SARS-CoV-2 vaccine candidate. *Nature*. 2021;590:320–325.
19 Li L-H, Liesenborghs L, Wang L, et al. Biodistribution and environmental safety of a live-attenuated YF17D-vectored SARS-CoV-2 vaccine candidate. *Mol Ther - Methods Clin Dev*. 2022;25:215–224.
20 Ma J, Boudewijns R, Sanchez-Felipe L, et al. Comparing immunogenicity and protective efficacy of the yellow fever 17D vaccine in mice. *Emerg Microbes Infect*. 2021;10:2279–2290.
21 Gaythorpe K, Abbas K, Huber J, et al. Impact of covid-19-related disruptions to measles, meningococcal a, and yellow fever vaccination in 10 countries. *Elife*. 2021;10:1–34.
22 Klitting R, Roth L, Rey FA, De Lamballerie X. Molecular determinants of Yellow Fever Virus pathogenicity in Syrian golden hamsters: one mutation away from virulence article. *Emerg Microbes Infect*. 2018;7:1–18.
23 Dallmeier K, Neyts J. Simple and inexpensive three-step rapid amplification of cDNA 5′ ends using 5′ phosphorylated primers. *Anal Biochem*. 2013;434:1–3.
24 Goldstein AL, McCusker JH. Three new dominant drug resistance cassettes for gene disruption in Saccharomyces cerevisiae. *Yeast*. 1999;15:1541–1553.
25 Goldstein AL, Pan X, McCusker JH. Heterologous URA3MX cassettes for gene replacement in Saccharomyces cerevisiae. *Yeast*. 1999;15:507–511.
26 Abdelnabi R, Boudewijns R, Foo CS, et al. Comparing infectivity and virulence of emerging SARS-CoV-2 variants in Syrian hamsters. *EBioMedicine*. 2021;68:103403.
27 Port JR, Yinda CK, Avanzato VA, et al. Increased small particle aerosol transmission of B.1.1.7 compared with SARS-CoV-2 lineage A in vivo. *Nat Microbiol*. 2022;7:213–223.
28 Sharma S, Vercruysse T, Sanchez-Felipe L, et al. Updated vaccine protects from infection with SARS-CoV-2 variants, prevents transmission and is immunogenic against Omicron in hamsters. *bioRxiv*. 2022; 2021.11.12.468374. [preprint].
29 Rasulova M, Vercruysse T, Paulissen J, et al. A high-throughput yellow fever neutralization assay. *Microbiology Spectrum*. 2022;10:e02548-21.
30 Boudewijns R, Thibaut HJ, Kaptein SJF, et al. STAT2 signaling restricts viral dissemination but drives severe pneumonia in SARS-CoV-2 infected hamsters. *Nat Commun*. 2020;11:1–10.
31 Dai L, Gao GF. Viral targets for vaccines against COVID-19. *Nat Rev Immunol*. 2021;21:73–82.
32 Harvey CE, Post JJ, Palladinetti P, et al. Expression of the chemokine IP-10 (CXCL10) by hepatocytes in chronic hepatitis C virus infection correlates with histological severity and lobular inflammation. *J Leukoc Biol*. 2003;74:360–369.
33 Wasmuth HE, Lammert F, Zaldivar MM, et al. Antifibrotic effects of CXCL9 and its receptor CXCR3 in livers of mice and humans. *Gastroenterology*. 2009;137:309–319.e3.
34 Tesh RB, Guzman H, Travassos Da Rosa APA, et al. Experimental yellow fever virus infection in the golden hamster (Mesocricetus auratus). I. Virologic, biochemical, and immunologic studies. *J Infect Dis*. 2001;183:1431–1436.
35 Julander JG, Trent DW, Monath TP. Immune correlates of protection against yellow fever determined by passive immunization and challenge in the hamster model. *Vaccine*. 2011;29:6008–6016.
36 Mok DZL, Chan KR. The effects of pre-existing antibodies on live-attenuated viral vaccines. *Viruses*. 2020;12:520.
37 Larocca RA, Abbink P, Ventura JD, et al. Impact of prior Dengue immunity on Zika vaccine protection in rhesus macaques and mice. *PLoS Pathog*. 2021;17:1–18.
38 Rodriguez-Barraquer I, Costa F, Nascimento EJM, et al. Impact of preexisting dengue immunity on Zika virus emergence in a dengue endemic region. *Science*. 2019;363:607–610.
39 Chan KR, Wang X, Saron WAA, et al. Cross-reactive antibodies enhance live attenuated virus infection for increased immunogenicity. *Nat Microbiol*. 2016;1:1–10.
40 Bradt V, Malafa S, von Braun A, et al. Pre-existing yellow fever immunity impairs and modulates the antibody response to tick-borne encephalitis vaccination. *npj Vaccines*. 2019;4:1–11.
41 Nohynek Hanna, Wilder-Smith Annelies. Does the World Still Need New Covid-19 Vaccines? *N Engl J Med*. 2022;22:2140–2142.
42 Massinga Loembé M, Nkengasong JN. COVID-19 vaccine access in Africa: Global distribution, vaccine platforms, and challenges ahead. *Immunity*. 2021;54:1353–1362.
43 Margolin E, Burgers WA, Sturrock ED, et al. Prospects for SARS-CoV-2 diagnostics, therapeutics and vaccines in Africa. *Nat Rev Microbiol*. 2020;18:690–704.
44 Çavdaroğlu S, Hasan MM, Mohan A, et al. The spread of Yellow fever amidst the COVID-19 pandemic in Africa and the ongoing efforts to mitigate it. *J Med Virol*. 2021;93:5223–5225.
45 Goldblatt D, Alter G, Crotty S, Plotkin SA. Correlates of protection against SARS-CoV-2 infection and COVID-19 disease. *Immunol Rev*. 2022.

46 Lustig Y, Sapir E, Regev-Yochay G, et al. BNT162b2 COVID-19 vaccine and correlates of humoral immune responses and dynamics: a prospective, single-centre, longitudinal cohort study in health-care workers. *Lancet Respir Med*. 2021;9:999–1009.

47 Saxena M, Van TTH, Baird FJ, Coloe PJ, Smooker PM. Pre-existing immunity against vaccine vectors - friend or foe? *Microbiol (United Kingdom)*. 2013;159:1–11.

48 Lauterbach H, Ried C, Epstein AL, Marconi P, Brocker T. Reduced immune responses after vaccination with a recombinant herpes simplex virus type 1 vector in the presence of antiviral immunity. *J Gen Virol*. 2005;86:2401–2410.

49 Roberts DM, Nanda A, Havenga MJE, et al. Hexon-chimaeric adenovirus serotype 5 vectors circumvent pre-existing anti-vector immunity. *Nature*. 2006;441:239–243.

50 Casimiro DR, Chen L, Fu T-M, et al. Comparative immunogenicity in rhesus monkeys of DNA plasmid, recombinant vaccinia virus, and replication-defective adenovirus vectors expressing a human immunodeficiency virus type 1 gag gene. *J Virol*. 2003;77:6305–6313.

51 Lemckert AAC, Sumida SM, Holterman L, et al. Immunogenicity of heterologous prime-boost regimens involving recombinant adenovirus serotype 11 (ad11) and ad35 vaccine vectors in the presence of Anti-Ad5 immunity. *J Virol*. 2005;79:9694–9701.

52 Barouch DH, Pau MG, Custers JHH V, et al. Immunogenicity of recombinant adenovirus serotype 35 vaccine in the presence of pre-existing anti-Ad5 immunity. *J Immunol*. 2004;172:6290–6297.

53 Pichla-Gollon SL, Lin S-W, Hensley SE, et al. Effect of preexisting immunity on an adenovirus vaccine vector: in vitro neutralization assays fail to predict inhibition by antiviral antibody in vivo. *J Virol*. 2009;83:5567–5573.

54 Ledgerwood JE, Costner P, Desai N, et al. A replication defective recombinant Ad5 vaccine expressing Ebola virus GP is safe and immunogenic in healthy adults. *Vaccine*. 2010;29:304–313.

55 Ramsauer K, Schwameis M, Firbas C, et al. Immunogenicity, safety, and tolerability of a recombinant measles-virus-based chikungunya vaccine: a randomised, double-blind, placebo-controlled, active-comparator, first-in-man trial. *Lancet Infect Dis*. 2015;15:519–527.

56 Reisinger EC, Tschismarov R, Beubler E, et al. Immunogenicity, safety, and tolerability of the measles-vectored chikungunya virus vaccine MV-CHIK: a double-blind, randomised, placebo-controlled and active-controlled phase 2 trial. *Lancet*. 2018;392:2718–2727.

57 Mok H. Evaluation of measles vaccine virus as a vector to deliver respiratory syncytial virus fusion protein or epstein-barr virus glycoprotein gp350. *Open Virol J*. 2012;6:12–22.

58 Lorin C, Mollet L, Delebecque F, et al. A single injection of recombinant measles virus vaccines expressing human immunodeficiency virus (HIV) type 1 clade B envelope glycoproteins induces neutralizing antibodies and cellular immune responses to HIV. *J Virol*. 2004;78:146–157.

59 Hadinegoro SR, Arredondo-García JL, Capeding MR, et al. Efficacy and long-term safety of a dengue vaccine in regions of endemic disease. *N Engl J Med*. 2015;373:1195–1206.

60 Villar L, Dayan GH, Arredondo-García JL, et al. Efficacy of a tetravalent dengue vaccine in children in Latin America. *N Engl J Med*. 2015;372:113–123.

61 McElrath MJ, De Rosa SC, Moodie Z, et al. HIV-1 vaccine-induced immunity in the test-of-concept Step Study: a case-cohort analysis. *Lancet*. 2008;372:1894–1905.